

EJONS

Uluslararası Matematik, Mühendislik ve Doğa Bilimleri Dergisi
International Journal on Mathematic, Engineering and Natural Sciences

Research Article

e-ISSN: 2602 - 4136

<https://doi.org/10.5281/zenodo.17998151>

Hirshfeld Surface Analysis and Intermolecular Interaction Profiling of Cyproheptadine Hydrochloride Sesquihydrate

Esra ÖZTÜRK ^{*}1, Seda GÜNEŞDOĞDU SAĞDINÇ ¹

¹Kocaeli University, Department of Physics, 41380 Kocaeli, Turkey
Corresponding Author Email: esra3.ozturk@gmail.com

Article Info

Received: 14.11.2025

Accepted: 18.12.2025

Keywords

Cyproheptadine
Hydrochloride,
Hirshfeld Surface
Analysis, Crystal
Structure, Van Der
Waals Interactions

Abstract: Cyproheptadine is a serotonin and histamine antagonist exhibiting notable anticholinergic and sedative properties. In the present study, Hirshfeld surface (HS) analysis and two-dimensional (2D) fingerprint plots were utilized to gain a deeper understanding of the intermolecular interactions governing the stability of the cyproheptadine hydrochloride sesquihydrate crystal. The HS analysis, performed using CrystalExplorer17.5, enabled visualization of interaction patterns within the crystal lattice through electron density partitioning, while the 2D fingerprint plots provided a quantitative assessment of atom–atom contact contributions. The findings demonstrate that hydrogen bonding interactions predominate and play a crucial role in maintaining the structural integrity and stability of the crystal, offering valuable insights for crystal engineering and pharmaceutical formulation studies.

1. Introduction

Cyproheptadine hydrochloride (CYP HCl, $C_{21}H_{21}N \cdot HCl \cdot 1.5H_2O$), chemically known as *4-(5H-dibenzo[a,d]-cyclohepten-5-ylidene)-1-methylpiperidine hydrochloride*, is a first-generation antihistaminic compound widely recognized for its sedative and antiserotonergic effects (Sweetman et al., 2002; Yamamoto et al., 2006; Feás et al., 2009a; Feás et al., 2009b; Feás et al., 2009c). The crystal structure of its hydrochloride sesquihydrate form has previously been characterized by Birknes (Birknes, 1977), revealing its distinct molecular packing. The chemical structure of cyproheptadine hydrochloride (CYP HCl) is shown in Figure 1. In addition to histamine H_1 receptor antagonism, CYP HCl exhibits serotonin receptor-blocking activity and calcium channel-modulating properties, particularly in smooth muscle and pancreatic islet cells. Due to its broad pharmacological profile, CYP HCl has been employed not only in the treatment of allergic disorders but also in certain endocrine conditions and for alleviating side effects associated with antidepressant medications (Sweetman et al., 2002).

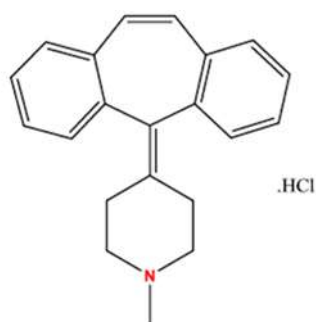


Figure 1. The chemical structure of cyproheptadine hydrochloride (CYP HCl)

Beyond its conventional antihistaminic use, cyproheptadine hydrochloride has demonstrated therapeutic efficacy in various neuropsychiatric disorders. Several studies have reported its effectiveness in reducing nightmares related to posttraumatic stress disorder (PTSD) (Feás et al., 2009a; Feás et al., 2009b). Moreover, it has been successfully used in the management of moderate to severe serotonin syndrome, a potentially life-threatening condition caused by excessive serotonergic activity. The drug's mechanism in this syndrome is attributed to dual antagonistic actions—blocking histamine H_1 receptors and inhibiting serotonin receptor subtypes 5-HT_{1A} and 5-HT_{2A}, both of which play crucial roles in mediating the symptoms of serotonin toxicity (Birknes, 1977; Yamamoto et al., 2006; Feás et al., 2009c). Structurally, only one crystalline salt form of cyproheptadine hydrochloride sesquihydrate has been reported so far in the Cambridge Structural Database (CSD entry: CYPHEP01), originally described by Birknes (Birknes, 1977). In this crystal form, the piperidine ring adopts a chair conformation and is double-bonded to a tricyclic aromatic framework, contributing to the molecular rigidity and solid-state stability of the compound.

In previous computational studies (Yoshida et al., 2014; Sağdıç et al., 2015), the molecular geometry, Mulliken charge distribution, natural bond orbital (NBO) characteristics, nonlinear optical (NLO) behavior, and vibrational frequencies of CYP HCl were investigated using both Hartree-Fock (HF) and density functional theory (DFT) methods. These analyses provided a solid theoretical basis for understanding the molecule's electronic and structural features, which now support the present crystallographic exploration.

The sesquihydrate nature of cyproheptadine hydrochloride is expected to play a significant role in its crystal packing behavior. Lattice water molecules can act as additional hydrogen-bond donors and acceptors, extending the intermolecular interaction network and contributing to a more balanced and stable crystal lattice. In contrast, a hypothetical anhydrous

form would lack such water-mediated bridging interactions, potentially resulting in a more limited hydrogen-bonding scheme and an alternative packing arrangement. Therefore, understanding the role of hydration is essential for a comprehensive interpretation of the crystal stability and intermolecular interactions of CYP HCl. Hirshfeld surface analysis is a powerful tool (Hirshfeld, 1977) for visualizing and quantifying intermolecular interactions in molecular crystals. This method extends the concept of the atomic weight function to describe not only individual atoms within a molecule but also the spatial boundaries of entire molecules in a crystalline environment. The isosurface, typically defined using a weight function $w(r) = 0.5$, encloses each molecule and partitions the crystal electron density to reveal the three-dimensional region dominated by a particular molecular unit. By incorporating contributions from both the central molecule and its surrounding atoms, this approach provides detailed insights into intermolecular interactions such as hydrogen bonding, van der Waals forces, and π - π stacking (Hirshfeld, 1977). Complementary two-dimensional (2D) fingerprint plots derived from these surfaces offer a quantitative visualization of the types and relative frequencies of intermolecular contacts, thereby enabling a deeper understanding of the crystal packing forces. Although cyproheptadine hydrochloride (CYP HCl) has been the subject of several pharmacological and computational studies, detailed crystallographic investigations such as Hirshfeld (Hirshfeld, 1977) surface or fingerprint plot analyses appear to be rather limited. Therefore, in this study, the intra and intermolecular interactions of CYP HCl were systematically examined through Hirshfeld surface and two-dimensional fingerprint plot analyses to elucidate the key factors governing its molecular packing and crystal stability.

2. Materials and Method

Cyproheptadine hydrochloride sesquihydrate ($C_{21}H_{21}N \cdot HCl \cdot 1\frac{1}{2}H_2O$) crystallizes in the orthorhombic crystal system (Figure 2.), space group Fdd2, with unit cell parameters $a = 43.53(1) \text{ \AA}$, $b = 18.226(6) \text{ \AA}$, $c = 9.578(4) \text{ \AA}$, and $Z = 16$. One water molecule is located on a twofold symmetry axis. The tricyclic core of the molecule is folded, with an angle of 124.1° between the planes of the two benzene rings. (Sağdınc et al., 2015). The piperidine ring adopts a chair conformation, while the seven-membered ring exhibits a boat conformation. The cyproheptadine molecule displays Cs symmetry within the experimental limits. The crystal structure was refined to an R-factor of 3.9%. The ring system can be approximately divided into two distinct planes, each defined by a benzene ring.

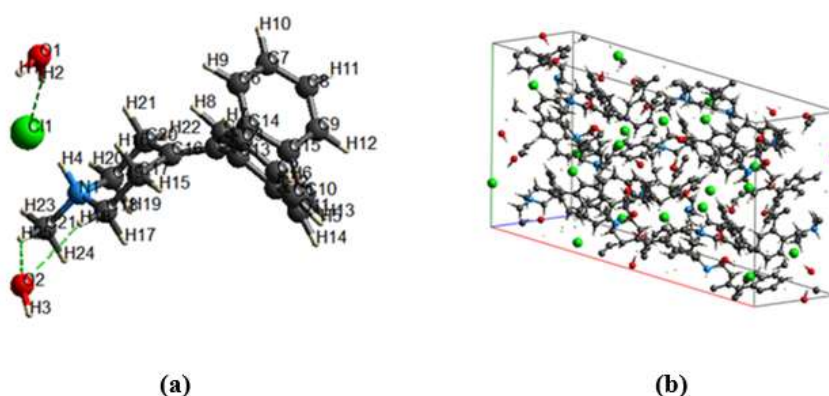


Figure 2. (a) The crystal structure, (b) crystal packing fragment (along a crystal axis) of Cyproheptadine hydrochloride sesquihydrate

A Hirshfeld surface (HS) analysis was performed using CrystalExplorer 17.5 to examine and visualize the intermolecular interactions present within the crystal structure of the title

compound (Moser et al., 1990; McKinnon et al., 2004). In this method, the distances from any point on the Hirshfeld surface to the nearest internal and external nuclei are expressed as d_i and d_e , respectively. The d_{norm} parameter, which provides a normalized measure of intermolecular contact distances, is calculated using d_i , d_e , and the van der Waals (vdW) radii of the involved atoms (Baylan et al., 2019).

$$d_{norm} = \frac{d_i - r_i^{vdW}}{r_i^{vdW}} + \frac{d_e - r_e^{vdW}}{r_e^{vdW}} \quad (1)$$

The d_{norm} surface has been visualized using a red–white–blue color scheme. Intermolecular contacts that are shorter than the sum of the van der Waals (vdW) radii are shown as red spots on the surface, indicating close interactions. Blue regions correspond to longer contacts, while white areas represent contacts approximately equal to the sum of the vdW radii.

The shape index (S) is a measure of the surface shape and is defined in terms of the principal curvatures κ_1 and κ_2 . It is given by Eq. (2):

$$S = \frac{2}{\pi} \arccos \left(\frac{\kappa_1 + \kappa_2}{\kappa_1 - \kappa_2} \right) \quad (2)$$

Curvedness (C) is a measure of how much curvature is present on the surface, and it is defined in terms of the principal curvatures κ_1 and κ_2 and given by Eq. (3).

$$C = \frac{2}{\pi} \ln \sqrt{\kappa_1^2 + \kappa_2^2} / 2 \quad (3)$$

Two-dimensional (2D) fingerprint plots were generated from the Hirshfeld surfaces to provide a visual and quantitative summary of the intermolecular contacts within the crystal structure (Spackman et al., 2002). These plots illustrate the frequency distribution of distance pairs d_e and d_i across the molecular surface by correlating these two parameters, the plots enable the identification of distinct types of intermolecular interactions and the estimation of the relative surface area associated with each contact type (Spackman et al., 2002).

In general, hydrogen bonding interactions dominate the overall pattern of these plots, typically appearing as two sharp, symmetric spikes extending toward the lower left region. The position and intensity of these spikes provide valuable information regarding the strength and nature of hydrogen bonds. Specifically, the upper spike (where $d_e > d_i$) represents the hydrogen bond acceptor region, while the lower spike (where $d_i > d_e$) corresponds to the donor region. In addition to hydrogen bonds, broad and diffuse regions in the plots signify van der Waals interactions and $H \cdots H$ contacts, while less frequent features may indicate $\pi \cdots \pi$ stacking or halogen-mediated interactions, depending on the molecular environment. Collectively, these 2D plots complement the 3D Hirshfeld surface visualization by quantifying and distinguishing the contributions of different interaction types to the overall crystal packing.

3. Results and Discussion

In the Hirshfeld surface (HS) (Figure 3) mapped over d_{norm} , the white regions indicate contacts with distances approximately equal to the sum of van der Waals (vdW) radii. Red regions represent closer-than-expected contacts (shorter than the vdW radii), indicating strong or close interactions, while blue regions correspond to longer contacts (distant interactions). Bright red spots observed near atoms H1, H2, H3, Cl1, and others highlight their involvement as donors or acceptors in the dominant C–H \cdots O and O–H \cdots Cl hydrogen bonding interactions. These oxygen and hydrogen atoms also appear as blue and red regions, respectively, on the electrostatic potential-mapped Hirshfeld surface, corresponding to positive and negative electrostatic potentials. In this mapping, blue regions indicate areas of positive electrostatic potential (typically hydrogen bond donors), whereas red regions correspond to negative potential zones (typically hydrogen bond acceptors). In this study, the molecular Hirshfeld surfaces, d_{norm} in the range of -0.5712 to 1.3458, d_e in the range of 0.7538 to 2.6295, d_i in the range of 0.7547 to 2.6255 of Cyproheptadine hydrochloride sesquihydrate are shown in Figure 3. As can be seen in Figure 3(a), d_{norm} map revealed significant red spots around electronegative atoms and hydrogen donors, which are indicative of hydrogen bonding interactions. Blue regions correspond to longer contacts, confirming the absence of close intermolecular interactions in these areas, while in Figure 3(b), d_i mapping highlighted regions of close proximity to the atomic cores. Small d_i values (blue) were concentrated around hydrogen atoms, whereas larger d_i values (green/yellow) were associated with bulkier substituents. This indicates steric crowding near hydrogen donors and also in Figure 3(c), d_e mapping demonstrated red areas around electronegative atoms, emphasizing short external contacts, while blue/green zones suggested less accessible regions. These results complement the d_i analysis and further confirm the dominance of hydrogen bonding.

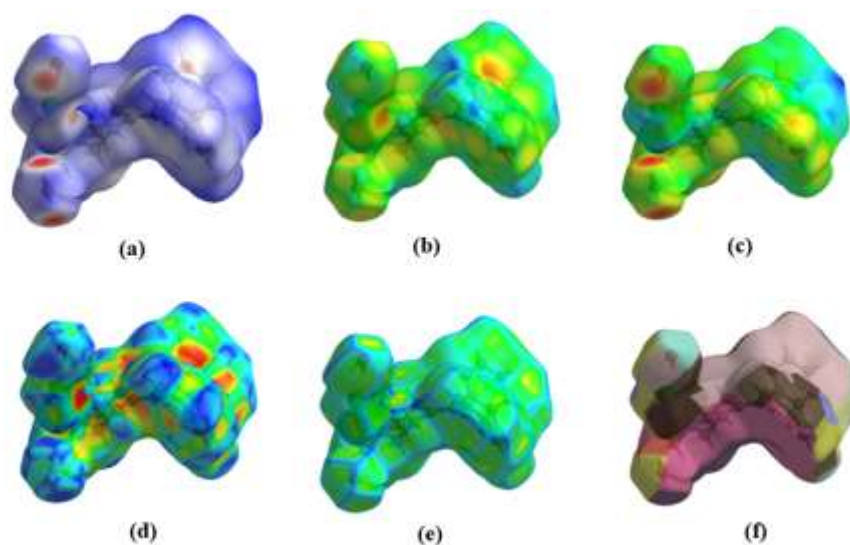


Figure 3. View of 3D Hirshfeld surface of the title complex plotted over (a) d_{norm} , (b) d_e , (c) d_i , (d) shape index, (e) curvedness and (f) fragment patch of the molecule.

The shape index and curvedness maps are useful tools for recognizing distinctive packing features within the crystal, including planar stacking motifs and the specific patterns by which neighboring molecules interact with each other (Baylan et al., 2019). Shape index mapped in the color range of -1.0000 to 1.0000, curvedness in the range of -4.0000 to 0.4000 and fragment patch in the range of 0 to 32.000 of Cyproheptadine hydrochloride sesquihydrate are shown in Figure 3. As can be seen in Figure 3(d), the shape index displayed alternating red and blue

patches on aromatic rings, characteristic of $\pi \cdots \pi$ stacking interactions. These face-to-face contacts are crucial in stabilizing layered arrangements in the crystal lattice. In Figure 3(e), the curvedness map identified large flat green regions, which are indicative of potential stacking interactions. Highly curved blue areas correspond to sterically hindered sites, reducing the likelihood of intermolecular overlap in these regions and in Figure 3(f), the fingerprint patch surface clearly separated different types of intermolecular contacts by color coding. Hydrogen \cdots hydrogen, hydrogen \cdots oxygen, and hydrogen \cdots halogen interactions were distinguished, highlighting their individual contributions to the overall crystal packing.

The two-dimensional (2D) representation of the Hirshfeld surface is known as the fingerprint plot (Figure 4). These plots can be decomposed to highlight specific atom-pair close contacts, defined by d_e and d_i , across the molecular surface. This allows not only the identification of different types of intermolecular interactions but also provides insight into the relative surface area associated with each interaction type. Hydrogen bonds are the dominant features in these plots, typically appearing as a pair of sharp spikes pointing toward the bottom left corner of the plot. In each case, the upper spike (where $d_e > d_i$) corresponds to a hydrogen bond donor, while the lower spike (where $d_e < d_i$) corresponds to a hydrogen bond acceptor (Baylan et al., 2019). The two-dimensional (2D) fingerprint plots (Figure 4a-j) provide a detailed visualization of the intermolecular contacts that govern the crystal packing of cyproheptadine hydrochloride sesquihydrate. As shown in Figure 4(a), the overall plot offers a global view of the crystal interactions. The dense blue region in the center and the two sharp downward spikes indicate that most points on the Hirshfeld surface are in close proximity to hydrogen atoms. This observation suggests that the crystal structure is primarily stabilized by hydrogen-involving interactions ($H \cdots H$, $H \cdots C$, $H \cdots Cl$, and $H \cdots O$), rather than a single dominant bonding motif. In Figure 4(b), the plot isolating the $Cl \cdots H/H \cdots Cl$ contacts reveals a distinct, narrow spike, characteristic of directional hydrogen bonds involving chlorine atoms. These interactions, typically observed in $N-H \cdots Cl$ or $O-H \cdots Cl$ motifs, exhibit a pronounced electrostatic component that contributes significantly to crystal cohesion, even though their overall surface contribution is moderate. The $O \cdots H/H \cdots O$ interactions, illustrated in Figure 4(c), appear as short spikes near the lower left region of the plot, confirming hydrogen bonds involving water molecules within the lattice consistent with the sesquihydrate nature of the compound. Their relatively small proportion indicates that only a limited number of water-mediated contacts locally reinforce the lattice structure. As depicted in Figure 4(d), the $O \cdots C/C \cdots O$ contacts are minimal, reflected by the nearly featureless fingerprint. This finding supports the role of oxygen atoms as hydrogen-bond acceptors rather than as participants in close carbon contacts, emphasizing their polar rather than dispersive contribution to the lattice. In Figure 4(e), the reciprocal $H \cdots Cl$ plot confirms the mutual participation of hydrogen and chlorine atoms in short, directional contacts, further validating the presence of a stable hydrogen-bonding network within the crystal. Similarly, Figure 4(f) presents the $H \cdots O$ interactions, which display a weaker but consistent pattern compared with Figure 4(c). These contacts are attributed to hydrogen atoms bonded to oxygen or nitrogen donors that interact with lattice water molecules, supporting the presence of a water-bridged hydrogen-bonding network. The dominant feature in Figure 4(g) corresponds to $H \cdots H$ interactions, accounting for approximately 56.4% of the total surface area. The broad and diffuse blue region reflects extensive van der Waals contacts between hydrogen atoms of neighboring molecules. Although individually weak, these numerous interactions collectively define the dense molecular packing typical of organic crystals. In Figure 4(h), the $H \cdots C/C \cdots H$ contacts ($\approx 10\%$) represent close approaches between hydrogen atoms and the aromatic carbon framework. The elongated blue streak suggests weak $C-H \cdots \pi$ and edge-to-face interactions that enhance lattice stabilization through dispersive forces. The contributions of $C \cdots O$ contacts in Figure 4(i) are negligible, indicating minimal overlap between carbon atoms and oxygen lone pairs. This finding

reinforces the idea that oxygen participates mainly in hydrogen bonding, with little involvement in π -O or dipolar interactions. Finally, the $C\cdots H$ contacts shown in Figure 4(j) display a broader and more diffuse distribution, representing multiple geometrically distinct approaches between carbon and hydrogen atoms. Together with $H\cdots C$ contacts, they contribute to efficient molecular packing and complement the overall hydrogen-bonding framework. Quantitatively, the decomposed fingerprint plots show that the crystal packing is stabilized by a balance between strong polar and weak dispersive interactions. $H\cdots H$ contacts (56.4%) dominate, reflecting the hydrogen-rich molecular surface. $H\cdots C$ and $C\cdots H$ interactions (≈ 21 – 22%) contribute to π -associated dispersion around the tricyclic aromatic system. The $H\cdots Cl/Cl\cdots H$ contacts (≈ 14 – 15%) and $H\cdots O/O\cdots H$ interactions ($\approx 7\%$) highlight the key structural roles of chloride anions and water molecules in forming hydrogen-bonding networks that anchor the lattice. The negligible contribution of $C\cdots O$ and $O\cdots C$ ($<1\%$) confirms that oxygen atoms act primarily as hydrogen-bond acceptors rather than engaging in nonpolar contacts.

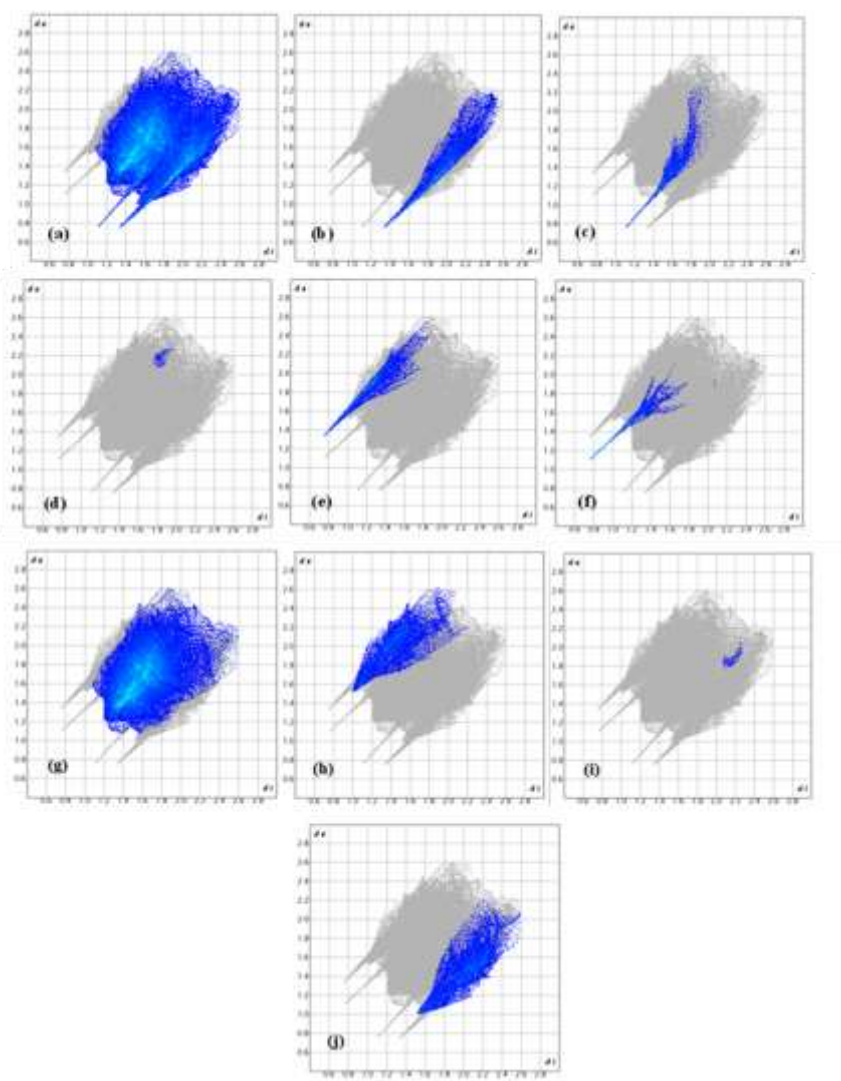


Figure 4. 2-D fingerprint plots of (a) all, (b) Cl-H, (c) O-H, (d) O-C, (e) H-Cl, (f) H-O, (g) H-H, (h) H-C, (i) C-O, (j) C-H interactions.

Overall, these findings demonstrate that the crystal packing of cyproheptadine hydrochloride sesquihydrate is dominated by hydrogen-mediated interactions, with chloride and water molecules serving as pivotal acceptor sites in the lattice. The combination of strong hydrogen bonds and complementary van der Waals and π -type interactions results in a stable,

compact molecular arrangement typical of pharmaceutically relevant organic salts. The percentage contributions of various intermolecular contacts obtained from the Hirshfeld surface analysis are summarized in Table 1.

Table 1. Percentage contributions of intermolecular contacts to the Hirshfeld surface of cyproheptadine hydrochloride sesquihydrate.

Contact Type	Interaction Symbol	Percentage Contribution (%)	Interaction Type
Hydrogen–Hydrogen	H···H	56,4	van der Waals
Hydrogen–Carbon	H···C	11,6	C–H··· π / dispersion
Carbon–Hydrogen	C···H	10,1	C–H··· π / dispersion
Hydrogen–Chlorine	H···Cl	9,2	Hydrogen bonding
Chlorine–Hydrogen	Cl···H	5,3	Hydrogen bonding
Hydrogen–Oxygen	H···O	3	Hydrogen bonding (via water)
Oxygen–Hydrogen	O···H	4	Hydrogen bonding (via water)
Oxygen–Carbon	O···C	0,1	Weak / negligible
Carbon–Oxygen	C···O	0,1	Weak / negligible

5. Conclusions

In this study, a comprehensive Hirshfeld surface and two-dimensional fingerprint plot analysis was performed on Cyproheptadine Hydrochloride Sesquihydrate to elucidate the key intermolecular interactions governing its crystal structure and stability. The analysis revealed that hydrogen bonding plays a dominant role in the molecular packing, supported by secondary van der Waals and $\pi\cdots\pi$ stacking interactions that contribute to the overall lattice cohesion. Specifically, H···H contacts accounted for more than half of the total surface contribution, confirming the hydrogen-rich environment of the molecule, while H···Cl and H···O interactions were identified as the major directional hydrogen bonds responsible for stabilizing the crystalline network through chloride anions and lattice water molecules. The 3D Hirshfeld surfaces, mapped over parameters such as d_{norm} , d_i , d_e , shape index, and curvedness, provided detailed visualization of close contacts, revealing the spatial distribution of electrostatic and dispersive interactions within the crystal lattice. The corresponding 2D fingerprint plots quantitatively decomposed these interactions, allowing the identification of dominant contact types and their relative contributions to crystal packing. These findings highlight the balance between strong polar and weak dispersive forces, which collectively ensure the structural robustness of the compound. The dominance of hydrogen bonding interactions, supported by lattice water molecules and complementary dispersive contacts, suggests that the sesquihydrate form of cyproheptadine hydrochloride possesses enhanced solid-state stability and a well-defined hydration environment, factors that are highly relevant for solid-form selection and pharmaceutical formulation. From a pharmaceutical standpoint, understanding the nature of these interactions provides valuable insights into the physicochemical behavior of Cyproheptadine Hydrochloride Sesquihydrate. The hydrate form, stabilized by hydrogen-bonding networks, is likely to exhibit enhanced storage stability and consistent bioavailability compared to its anhydrous counterparts. Therefore, the present results not only contribute to a deeper understanding of the crystallographic characteristics of CYP HCl Sesquihydrate but also provide a structural foundation for rational drug design, solid-form selection, and quality control in pharmaceutical formulations.

Declaration of Author Contributions

All authors declare that they have contributed equally to this manuscript, have reviewed the final version, and have approved it for publication.

Declaration of Conflicts of Interest

The authors declare that there is no conflict of interest regarding this study.

References

- Baylan, D., Sağdıncı, S.G., 2019. Hirshfeld surface analysis of diclofenac acid. *AIP Conference Proceedings*, 2178: 030029.
- Birknes, B., 1977. The structure of an antihistamine: cyproheptadine hydrochloride sesquihydrate, *Acta Crystallographica*, B33: 687-691.
- Feás, X., Ye, L., Regal, P., Fente, C.A., Hosseini, S.V., Cepeda, A., 2009a. Application of dummy molecularly imprinted solid-phase extraction in the analysis of cyproheptadine in bovine urine. *Journal of Separation Science*, 32: 1740-1747.
- Feás, X., Seijas, J.A., Vázquez-Tato, M.P., Regal, P., Cepeda, A., Fente, C., 2009b. Syntheses of molecularly imprinted polymers: Molecular recognition of cyproheptadine using original print molecules and azatadine as dummy templates. *Analytica Chimica Acta*, 631: 237-244.
- Feás, X., Fente, C.A., Hosseini, S.V., Seijas, J.A., Vázquez, B.I., Franco, C.M., Cepeda, A., 2009c. Use of acrylic acid in the synthesis of molecularly imprinted polymers for the analysis of cyproheptadine. *Materials Science and Engineering C*, 29: 398-404.
- Hirshfeld, F.L., 1977. Bonded-atom fragments for describing molecular charge densities. *Theoretical Chemistry Accounts*, 44: 129-138.
- McKinnon, J.J., Spackman, M.A., Mitchell, A.S., 2004. Novel tools for visualizing and exploring intermolecular interactions in molecular crystals. *Acta Crystallographica*, B60: 627-668.
- Moser, P., Sallman, A., Weisemberg, I., 1990. Synthesis and quantitative structure-activity relationships of diclofenac analogs. *Journal of Medicinal Chemistry*, 33: 2358-2368.
- Sağdıncı, S.G., Erdaş, D., Gündüz, I., Şahintürk, A.E., 2015. FT-IR and FT-Raman spectra, molecular structure and first-order molecular hyperpolarizabilities of a potential antihistaminic drug, cyproheptadine HCl. *Spectrochimica Acta, Part A: Molecular and Biomolecular Spectroscopy*, 134: 350-360.
- Spackman, M.A., McKinnon, J.J., 2002. Fingerprinting intermolecular interactions in molecular crystals. *CrystEngComm*, 4: 378-392.
- Sweetman, S.C., 2002. Martindale-The Complete Drug Reference (33rd Ed.). Pharmaceutical Press, London.
- Yamamoto, Y., Niwa, S., Iwayama, S., Koganei, H., Fujita, S., Takeda, T., Kito, M., Ono, Y., Saitou, Y., Takahara, A., Iwata, S., Yamamoto H., ShojiBioorg, M., 2006. Discovery, structure activity relationship study, and oral analgesic efficacy of cyproheptadine derivatives possessing N-type calcium channel inhibitory activity. *Medical Chemistry*, 14: 5333-5339.
- Yoshida, T., Mashima, A., Sasahara, K., Chuman, H., 2014. A simple and efficient dispersion correction to the Hartree-Fock theory. *Bioorganic & Medicinal Chemistry Letters*, 24(4): 1037-1042.